Journal of Cell Science 107, 1783-1796 (1994)
Printed in Great Britain © The Company of Biologists Limited 1994

The mode of anchorage to the cell surface determines both the function and the membrane location of Thy-1 glycoprotein

M.-C. Tiveron[1], M. Nosten-Bertrand[1], H. Jani[1], D. Garnett[4], E. M. A. Hirst[2], F. Grosveld[3] and R. J. Morris[1,*]

Laboratories of [1]Neurobiology (Norman and Sadie Lee Centre), [2]Eukaryotic Molecular Genetics and [3]Gene Structure and Expression, National Institute for Medical Research, The Ridgeway, Mill Hill London NW7 1AA, UK
[4]Cellular Immunology Unit, Sir William Dunn School of Pathology, Oxford OX1 3RE, UK

*Author for correspondence

SUMMARY

The surface glycoprotein, Thy-1, when expressed by transfection in NG115/401L neural cells, inhibits their neurite outgrowth over astrocytes. We have investigated the role of the glycosylphosphatidylinositol anchor of Thy-1 in this inhibition. Hybrid molecules, in which the lipid anchor was replaced by polypeptide transmembrane domains, were expressed by transfection. Lines expressing Thy-1 with the transmembrane and full cytoplasmic domains of NCAM-140, or with the transmembrane and truncated cytoplasmic domain of CD8, were not inhibited in their ability to extend neurites over astrocytes. Truncation of the cytoplasmic domain of NCAM-140 to just two amino acids, however, produced a transmembrane form of Thy-1 that, when expressed at high levels, inhibited neurite outgrowth. All forms of Thy-1 were concentrated in clusters that occurred primarily on fine filopodia. In double transfectants expressing normal Thy-1 and Thy-1 with the full NCAM cytoplasmic tail, the clusters of each form were separate, with no instances of the transmembrane form being found within the clusters of lipid-anchored Thy-1. Thy-1 with the two-amino-acid cytoplasmic domain of NCAM also occurred in clusters separate from those occupied by lipid-anchored Thy-1, but substantial 'invasion' of the clusters of normal Thy-1 by this transmembrane construct occurred. We suggest that the ability of this hybrid protein to enter the lipid-anchored clusters enables it to activate the signalling pathways that normal Thy-1 uses. Thus the membrane anchor, in targetting Thy-1 to different microdomains on the cell surface, determines its ability to inhibit neurite outgrowth on astrocytes.

Key words: astrocyte, CD8, cell surface, glycosylphosphatidylinositol, NCAM, neurite outgrowth, transmembrane domain

INTRODUCTION

A diverse group of proteins, including enzymes, receptors and adhesion molecules of the immunoglobulin (Ig) and fibronectin type III superfamilies, are anchored to the cell surface, not by a conventional transmembrane polypeptide domain but by a glycosylphosphatidylinositol (GPI) group (e.g. see Ferguson, 1992; Walsh and Doherty, 1992). Two lines of research have recently converged to suggest that GPI anchors are not inert membrane tethers, but actively confer upon proteins the ability to act as receptors or transporters, conveying signals or metabolites across the membrane that they themselves do not span (Hooper, 1992).

The GPI-anchored proteins of lymphocytes, when cross-linked with antibody, rapidly stimulate an influx of Ca^{2+}, inositol phosphate turnover, and specific patterns of protein phosphorylation, leading to cytokine release and finally mitosis (Robinson, 1991). This property is eliminated if the GPI-anchor is replaced by a conventional polypeptide transmembrane anchor; conversely, substitution of a transmembrane polypeptide anchor (on class I major histocompatibility antigen) for a GPI-anchor confers upon the histocompatibility antigen the ability to activate lymphocytes (Robinson et al., 1989; Su et al., 1991). Immunoprecipitation of GPI-anchored proteins from mild, non-denaturing detergent extracts of lymphocytes co-precipitates protein kinase (Stefanova et al., 1991; Shenoy-Scaria et al., 1992; Thomas and Samelson, 1992) and phosphatase activity (Volarevic et al., 1990), suggesting that these signal-transducing molecules are associated with the GPI-linked proteins. Substitution of a transmembrane for a GPI anchor on decay accelerating factor removes this association, so that tyrosine kinase activity no longer co-precipitates with the surface protein (Shenoy-Scaria et al., 1992). It remains to be proven that this mechanism is physiologically relevant, since no endogenous ligand-GPI protein interaction has been described that mimics the effect produced by antibodies.

The second approach that suggests a functional link between the GPI anchor and transmembrane communication comes from studies of specialised microdomains on the cell surface, the caveolae, into which a number of GPI-anchored proteins are clustered (Ying et al., 1992). In addition, certain cell surface proteins that have conventional transmembrane

domains (e.g. Ca^{2+} channels; Fujimoto, 1993; Fujimoto et al., 1993) and various intracellular signalling molecules (Sargiacomo et al., 1993) are also highly enriched in these structures, so creating a surface organelle that is specialised for transmembrane communication (Anderson, 1993). The GPI-anchor could direct proteins to these microdomains by interactions with specific lipids, in particular cholesterol, that are enriched in these areas (Rothberg et al., 1990a; Hooper and Bashir, 1991; Brown, 1992; Lisanti et al., 1993; Zurzolo et al., 1994).

The role of the GPI group, therefore, might be to direct the proteins that it anchors to particular functional microdomains on the cell surface. If this is the case, substitution of the GPI anchor by transmembrane polypeptide domains should influence both the microdomain occupied by the protein on the cell surface and its function. Here, we investigate this hypothesis using Thy-1. This major component of the surface of mature neurons (and some other cell types) occurs naturally only as a GPI-anchored protein (Williams, 1989), giving a clear background against which to assess the contribution of constructed transmembrane forms. Its polypeptide chain folds into a single Ig variable-type domain, a stable structure (Williams et al., 1989) that in Thy-1 is further reinforced by two disulfide bonds. The structure of its GPI anchor (Homans et al., 1988) is known, and well-characterised antibodies to its polypeptide chain are available.

During development, Thy-1 appears on axons only after they have finished growth, suggesting that the molecule might participate in stabilising axonal networks, possibly by down-regulating growth (Morris, 1992; Xue and Morris, 1992). We tested this possibility with transfected clones from the neural cell line, NG115/401L. We found that Thy-1 inhibits neurite extension over mature astrocytes, but not over other cell types, including those glial cells that support axonal growth in vivo. The properties of this interaction strongly suggest that the binding of an astrocytic ligand to Thy-1 directly signals an inhibition of neurite outgrowth in the neural cells (Tiveron et al., 1992; Morris, 1992).

This assay is both simple and sensitive; we found effective inhibition of neurite outgrowth by clones differing 20-fold in their levels of surface Thy-1 (Tiveron et al., 1992). We have therefore used this assay to determine how substitution of transmembrane polypeptide domains for the GPI-anchor of Thy-1 affects its ability to inhibit neurite outgrowth over astrocytes, and related this to the distribution of the various forms of Thy-1 on the plasma membrane.

MATERIALS AND METHODS

Construction of transmembrane forms of Thy-1

To link Thy-1 to different transmembrane domains, a *Stu*I site was created after the codon for Cys112, the carboxy-terminal amino acid of normal Thy-1 (and that to which the GPI anchor is attached; Williams, 1989). The Ser116 codon, AGC, was changed to GGC (Gly) by oligonucleotide-directed mutagenesis using the polymerase chain reaction (PCR). Different transmembrane constructs were then inserted between this *Stu*I and the downstream *Xho*I site of the Thy-1 gene to replace the segment encoding the transient transmembrane domain of Thy-1 whose removal triggers GPI addition.

A 0.2 kb *Eco*RV-*Sal*I fragment from pLy-2a′.RVxpUC (Zamoyska et al., 1989) encoding the transmembrane domain of CD8 with its cytoplasmic domain truncated to just three amino acids was ligated to a small fragment of two complementary oligonucleotides (5′-CCT-GAGCGAT-3′ and 5′-ATCGCTCAGG-3′) at the *Eco*RV end, enabling the sequences to be joined in frame via a peptide hinge between the Ig domain of Thy-1 and the transmembrane domain of CD8 (Fig. 1, 'Thy-1-CD8').

A blunt-ended *Stu*I-*Asp*718 0.4 kb fragment (from pRB7; Small et al., 1987) encoding the transmembrane and full cytoplasmic domains of rat NCAM-140 was similarly inserted in frame into the *Stu*I site to produce Thy-1-NCAM (Fig. 1). Truncated versions of the NCAM fragment carrying TGA stop codons (introduced by PCR using appropriate oligonucleotide primers) replacing two Cys and one Gly codon, respectively (Fig. 1, underlined residues in Thy-1-NCAM), were also made and inserted. Two of these produce viable hybrid proteins, termed Thy-1-NC28s (with the first 28 amino acids of NCAM's cytoplasmic domain) and Thy-1-NC2s (first 2 cytoplasmic amino acids of NCAM). The final NCAM-based construct terminates within the transmembrane domain, at the Thr residue that is four amino acids in from the cytoplasmic face (Fig. 1). The integrity of all constructs was verified by sequencing.

The human Thy-1 coding region was obtained from the mhm Thy-1 construct (Vidal et al., 1990). The expression of these normal and recombinant Thy-1 genes was driven by the human β-actin promoter as described previously (Tiveron et al., 1992). A 1.1 kb *Xho*I-*Sal*I fragment from pMC1-Neo containing the neomycin resistance gene regulated by the thymidine kinase promoter was added to the final constructs before use.

Antibodies

The mouse Thy-1-based constructs were detected using either H129-93 (Pont et al., 1985) or 30H12 (Ledbetter and Herzenberg, 1979) monoclonal antibodies to the Thy-1.2 allelic determinant specified by a Gln residue at position 89 (Williams, 1989). H129-93 IgG, digested with pepsin, gave Fab antibody fragments (rather than the expected F(ab)′$_2$) that eluted from Sephacyl S-300 (Pharmacia) at M_r 50,000; these were biotinylated with NHS-LC-Biotin (Pierce: 1 mg/18.4 mg Fab). In addition, ascitic fluid of monoclonal antibodies to two other epitopes on Thy-1 (H140-150 (against the 'B' epitope), and H154-177, H154-200 and H155-124 (against the 'C' epitope)) were used (Pont et al., 1985). Human Thy-1 was detected with the B7 clone; it does not cross-react with mouse Thy-1(Miyata et al., 1990). Rabbit anti-rat Thy-1 F(ab)′$_2$ antibodies (Morris et al., 1983) detect Thy-1 from all mammalian species, and in reduced and unreduced form in immunoblots, providing a general Thy-1 detection system. They were absorbed with deoxycholate-solublised rat brain membrane proteins (immobilised to Pierce AminoLink gel) from which Thy-1 had been removed by immunoaffinity chromatography prior to use. Immunoaffinity-purified, species-specific sheep F(ab′)$_2$ anti-rabbit F(ab′)$_2$, coupled to FITC or HRP, were as described (Morris et al., 1983).

Transfection, selection and validation of clones

NG115/401L cells (2×10^7/ml in 140 mM NaCl, 25 mM HEPES, pH 7.5, 0.75 mM Na_2HPO_4) were transfected with 10 μg of linearised plasmid by electroporation (960 μF at 250 mV in a Bio-Rad Gene Pulser), and cultured in 5% fetal calf serum/HXXI medium. For dual transfection, 1 μg of linearised plasmid containing the human Thy-1 and neomycin-resistance genes was mixed with 10 μg of fragment encoding the appropriate transmembrane Thy-1. Clones emerging after selection in 1-1.5 mg/ml G418 were isolated with cloning rings. Their Thy-1 expression was assessed by flow cytometry on a Becton Dickinson FacStar following saturating labelling for Thy-1 (rat antibodies of either 30H12 or H129-93 clones at 2 μg/10^6 cells per ml followed by FITC-coupled rabbit anti-rat IgG (Dako; 1:20 dilution)). The proportion of Thy-1-expressing cells was screened routinely by flow cytometry, and where necessary the expressing population was purified by sorting before analysis for function or surface distribution.

Phosphatidylinositol-specific phospholipase C (PI-PLCase) treatment

The presence of a GPI linkage was assessed by comparing the intensity of Thy-1 immunofluorescent labelling of cells incubated for 1 hour at 37°C with, or without, PI-PLCase (700 milliunits/ml in serum-free HXXI medium; *Bacillus cereus* enzyme from Boehringer Mannheim). For assessing the effect of PI-PLCase treatment on neurite outgrowth, cells were incubated for 45 minutes in 1 unit/ml of recombinant *Bacillus thuringiensis* enzyme (Oxford GlycoSystems Ltd); a sample was removed for flow cytometric analysis, the remaining cells were labelled with dye and assayed for neurite outgrowth.

Immunoblot analysis of Thy-1 forms

For immunoblot analysis, cells (approximately 10^7 cells in 100 μl of PBS) were pipetted into 1.2 ml of non-reducing Laemmli (1970) sample buffer containing 5 mM iodoacetamide and 5 mM EDTA, pre-equilibrated in a boiling water bath. Phenylmethylsulphonyl fluoride (15 μl of 100 mM solution in dried ethanol) was immediately added and mixed by pipetting, and the mixture was left in the water bath for 2 minutes before being mildly sonicated to disrupt the DNA. Samples were electrophoresed in 12% acrylamide gels and transferred to nitrocellulose membranes on which Thy-1 was visualised using rabbit anti-Thy-1 $F(ab)'_2$ at 0.5 μg/ml followed by HRP-coupled $F(ab')_2$ sheep anti-rabbit $F(ab')_2$ and the NEN Renaissance chemiluminescence reagent. The expected molecular mass in SDS-PAGE of the transmembrane constructs can be calculated by adding to the value for normal Thy-1 (25-29 kDa), the contribution from the transmembrane and cytoplasmic domains (Thy-1-NCAM, 16 kDa; Thy-1-NC28s, 6.6 kDa; Thy-1-NC2s and Thy-1-CD8, 3.8 kDa; Thy-1-NCms, 3.1 kDa) less any contribution from the GPI group.

Assay of neurite outgrowth over astrocytes

This was as described (Tiveron et al., 1992). Total neurite outgrowth for individual cells was determined using Fluorovision software (ImproVision, Coventry UK) with a Hamamatsu C3077 CCD camera; the image for each cell was checked down the microscope under fluorescence and phase-contrast optics (the latter to establish that the cell was on the astrocyte layer).

Fixation for immunolocalization

Cells were fixed and immunolabelled at 0-4°C when still in their culture dishes. Fixation (15 minutes, 0.1 M phosphate buffer, pH 7.4) was with 1% paraformaldehyde plus 0.05% glutaraldehyde (Taab Laboratories, EM grade), or for fluorescence microscopy with 1.5% paraformaldehyde. Free aldehydes were quenched with 0.153 M ethanolamine-Cl, pH 8.5. To permeabilise cells, a 10 minute incubation on a tilting plate at 4°C with 0.1% saponin or 0.3% Triton X-100 was included in certain experiments. The fixation conditions were selected after testing the range of conditions that we previously investigated for rat Thy-1 (Morris and Barber, 1983); they preserve over 85% of Thy-1 antigenicity (tested for normal GPI-linked mouse and human Thy-1, and Thy-1-NCAM).

Immunohistochemistry

For mouse Thy-1, cells were incubated with 20 μg/ml of biotin-labelled H129 Fab for 20 minutes at 4°C on a tilting plate, washed and then incubated for 40 minutes with either 1 nm streptavidin-gold (BioCell Research Laboratories, Cardiff; 1:20), or FITC-avidin (Vector Laboratories; 1:5000). Fluorescent samples were observed with a Bio-Rad MRC 600 confocal microscope with an argon/krypton laser. Gold-labelled samples were further fixed at room temperature for 1 hour in 2.5% glutaraldehyde/1% paraformaldehyde, washed repeatedly in 250 mM sucrose/20 mM HEPES, pH 7.4, and the gold particles were enlarged using silver lactate/*N*-propyl gallate for 15-20 minutes (Burry et al., 1992). One drawback of this procedure was that the embedding resin tended to tear away from the silver-coated gold, particularly where it was clustered at high density; this rarely obscured the pattern of labelling.

For double labelling, cells were incubated with 20 μg/ml B7 anti-human Thy-1 antibodies, then with 10 nm anti-mouse Ig-gold (BioCell, mean diameter 10.8 nm, coefficient of variation 5.9%) or Texas Red-labelled affinity-purified goat anti-mouse IgG (Calbiochem, 1:40), followed by a 10 minute incubation with 1% mouse and 1% rat serum in PBS before being incubated with biotin-H129 Fab (in 1% rat serum in PBS) and finally 5 nm avidin-gold (BioCell, mean diameter 5.5 nm, coefficient of variation 9.4%) or FITC-avidin as above. For analysis in the confocal microscope, aperture settings were adjusted using cells singly labelled with each fluorochrome to obtain less than 1.5% bleed-through into the other channel (assessed using the LEN program in the SOM software, on 3-5 intensely labelled cells).

For electron microscopy, the cell monolayers, stained for 15-20 minutes in 1% OsO_4 and aqueous 1% uranyl acetate, were scored into 0.5 mm squares before the plastic dish was dissolved in propylene oxide. The squares were transferred to flat-bottomed polypropylene centrifuge tubes, washed extensively with propylene oxide before being left overnight in a 1:1 mixture with Araldite CY212. The cell layers were centrifuged together at 2,000 ***g*** for 10 min before polymerisation. Grids, conventionally stained, were viewed in a Jeol 100CX.5.

The density of gold labelling was measured from photographs (×20,000) of the perimeter of single cells traced onto a graphics tablet (Bit Pad Two, Summagraphics Corp, Ct) measured using Digit (B.P. Hayes Image Analysis Software, Berkhampsted, UK); gold particles were counted in a dissecting microscope.

RESULTS

Rationale for the design of suitable transmembrane forms of Thy-1

We needed a functionally inert polypeptide sequence to replace the GPI group that provides both a flexible extracellular linker and a membrane anchor. Two proteins (CD16, the Fc γ RIII receptor; and CD58, better known as LFA-3) have Ig-type domains immediately adjacent to the plasma membrane, and occur in both GPI- and transmembrane-anchored forms. A linker region of five (CD16; Ravetch and Kinet, 1991) or seven (CD58; Dustin and Springer, 1991) amino acids replaces the GPI moiety in the transmembrane forms, suggesting that this number of amino acids can form a GPI-equivalent linker. We therefore designed hinge regions of seven (CD8) or eight (NCAM) amino acids, including three/four Gly residues to promote flexibility, by using three residues from the Thy-1 transient transmembrane domain (removed when the GPI anchor is inserted) and the last five extracellular amino acids of NCAM, or the last extracellular residue of CD8 with three further residues (coded by linking oligonucleotides) equivalent to those in NCAM (Fig. 1).

The transmembrane domain with a truncated cytoplasmic portion of the lymphocyte protein, CD8, was expected to be functionally neutral in neural cells. Its cytoplasmic domain of just three residues contains the basic amino acids that define the end of the transmembrane domain (Cramer et al., 1992), but lacks the functional motif (cytoplasmic residues 6-18 of CD8) that interacts with the tyrosine kinase $p56^{lck}$ (Shaw et al., 1990). Constructs based on the transmembrane/cytoplasmic domains of NCAM-140 might show a functional contribution from the NCAM portion, since the transmembrane forms of NCAM (-140 and -180) can signal intracellularly and promote

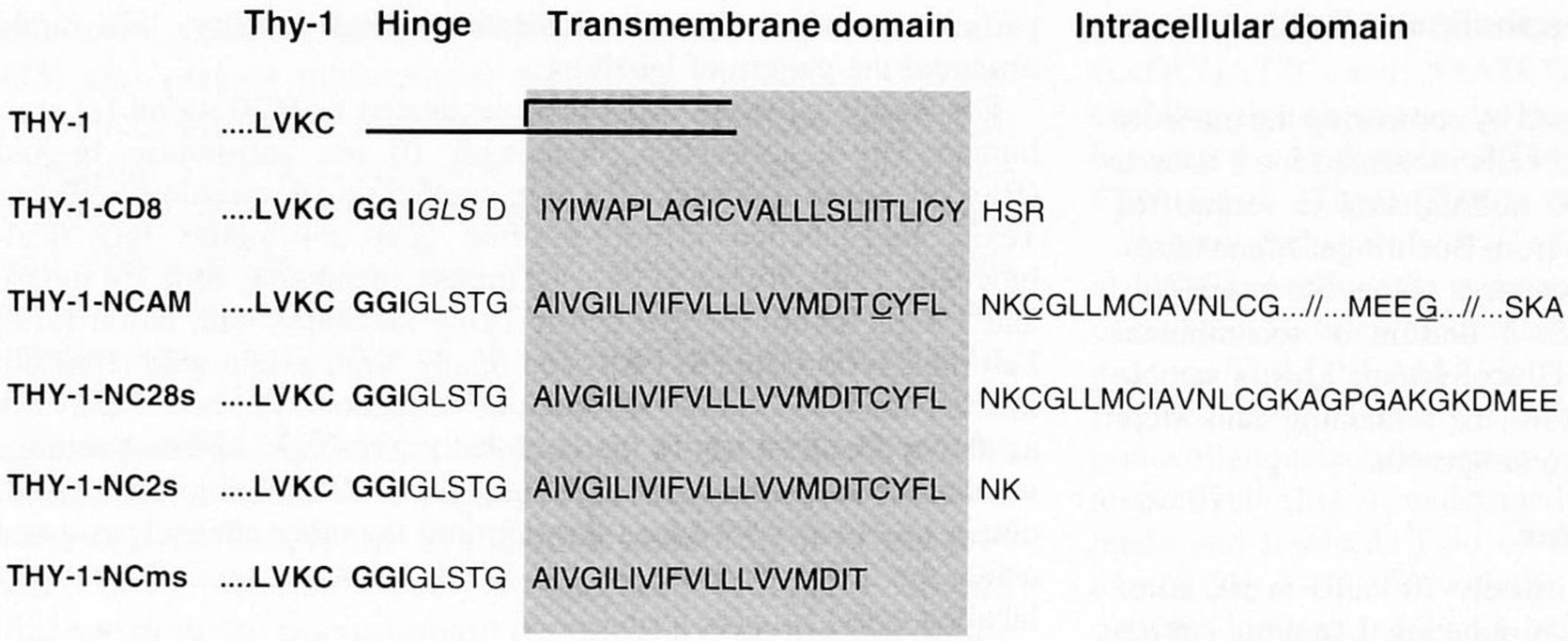

Fig. 1. Amino acid sequence (single letter code) of the Thy-1 constructs used for the extracellular hinge region, transmembrane and cytoplasmic domains. The GPI anchor of Thy-1 is shown schematically; residues in the hinge region derived from Thy-1 are in bold, those derived from NCAM or CD8 are in plain type; residues in italics (Thy-1-CD8) were encoded by linking oligonucleotides. Underlined residues in Thy-1-NCAM are those whose codons were converted to TGA stop codons to make the NC constructs.

axonal growth (Doherty and Walsh, 1992). To neutralise the cytoplasmic domain, we truncated it, in Thy-1-NC2s, to the minimum required structurally. In addition, NCAM is acylated (Cunningham et al., 1987), a post-translational modification that influences the microenvironment occupied by a protein within the membrane (O'Dowd et al., 1989; Parenti and Magee, 1994). The cytoplasmic Cys residues immediately adjacent to the membrane are potential palmitoylation sites (Parenti and Magee, 1994) and are included in the truncated cytoplasmic domain of Thy-1-NC28s (Fig. 1).

Our assignment of the transmembrane domain of NCAM differs from that shown in the original publications (Cunningham et al., 1987; Dickson et al., 1987; Santoni et al., 1987; Small et al., 1987), which started the transmembrane domain with the G that we assign to being the last extracellular residue, and terminated it 17 residues later at M, making D (aspartate) the first intracellular amino acid (see the NCAM sequence in Fig. 1). It has since become clear that this suggested transmembrane domain lacks crucial features characteristic of eukaryotic type 1 transmembrane domains, which are 20-26 amino acids in length, with one or more basic juxta-membrane cytoplasmic residues (K,R,H), and, less stringently, aromatic (F,W,Y) and larger aliphatic (L, I) residues within the membrane domain near the cytoplasmic face (see e.g. the CD8 sequence in Fig. 1; and Barclay et al., 1993; Jones et al., 1994; Sipos and Heijne, 1993). We tested the published NCAM domain on a program designed to identify the structure and orientation of transmembrane domains (Jones et al., 1994); it was given a rating of −1.237 nats (nats is a statistical unit of information content expressed as a natural logarithm; Robson and Suzuki, 1976), well below the range for transmembrane domains. The program identified the longer transmembrane sequence shown in Fig. 1 as the optimal transmembrane domain for NCAM, with a high nats score of 12.987. The Thy-1-NCms construct was designed to differentiate between the two assignments. If the earlier assignment of the short transmembrane domain is correct then Thy-1-NCms should be expressed. If, however, our assignment is correct, then Thy-1-NCms should be unstable and degraded as it is synthesised on the endoplasmic reticulum (Lankford et al., 1993).

Establishment of stably transfected lines expressing Thy-1 with different forms of membrane anchor

For simplicity, we will define a cell line by the name of the Thy-1 form produced, followed by its clone number. We took for our normal (GPI-anchored) Thy-1-expressing cells the highest and lowest expressing lines used in the previous study (Tiveron et al., 1992), where they were called M1 and H1; we refer to them here as lines Thy-1/9 and Thy-1/6, respectively. We included as a third normal Thy-1 control the line Thy-1/3, expressing 70% the Thy-1/9 level (Table 1).

The form of Thy-1 on the different clones was assessed by immunoblotting. With the exception of Thy-1-NCms, clones expressing the transmembrane constructs produced a single immunoreactive band, of molecular mass 29.5 kDa for Thy-1-NC2s and Thy-1-CD8, 32 kDa for Thy-1-NC28s, and 46-48 kDa for Thy-1-NCAM, compared to 26 kDa for native Thy-1 on Thy-1/3 cells, or 28 kDa from mouse brain (Fig. 2 and data

Table 1. Neurite outgrowth over astrocytes by transfected cells expressing different forms of Thy-1

Thy-1 variants	Clone	% Thy-1 expression*	% Outgrowth (mean ± s.d.)†	Growth inhibited‡
Nil	NG115	0	69.4±8.1	No
Thy-1	/9	100	26.5±4.9	Yes
	/3	70	22.3±7.2	Yes
	/6	5	23.7±3.8	Yes
Thy-1-NCAM	/1	75	60.8±4.0	No
	/3	50	64.4±6.5	No
	/5	25	68.3±5.4	No
	/8	25	67.4±10.6	No
Thy-1-NC28s	/1	75	77.8±7.3	No
	/10	65	57.1±6.6	Partial
Thy-1-NC2s	/1	75	47.2±10.	Partial
	/2	25	64.2±11.1	No
	/3	75	46.1± 4.4	Partial
	/5	30	68.7±10.1	No
	/Hi	115	33.6±13.2	Yes
	/Lo	30	57.5±2.3	Partial
Thy-1-CD8	/4	30	63.3±7.8	No
	/9	60	63.9±10.2	No
	/10	70	64.5±3.1	No

*Mean level of surface Thy-1, determined by FACS analysis of immunolabelled living cells, compared with level on Thy-1/9 cells.

†For clones expressing transmembrane Thy-1, 4-7 assays were done, although for negative cells (401L) and normal Thy-1-expressing cells (Thy-1/9 and /3) the number of assays were 44, 11 and 18, respectively.

‡No and Yes indicate that the % of cells extending neurites was not significantly different ($P \geq 0.05$) than that of NG115/401L or Thy-1/9 cells, respectively; Partial indicates that the % of cells extending neurites differed from both at $P \leq 0.001$. Significance was determined by *t*-test using SuperAnova.

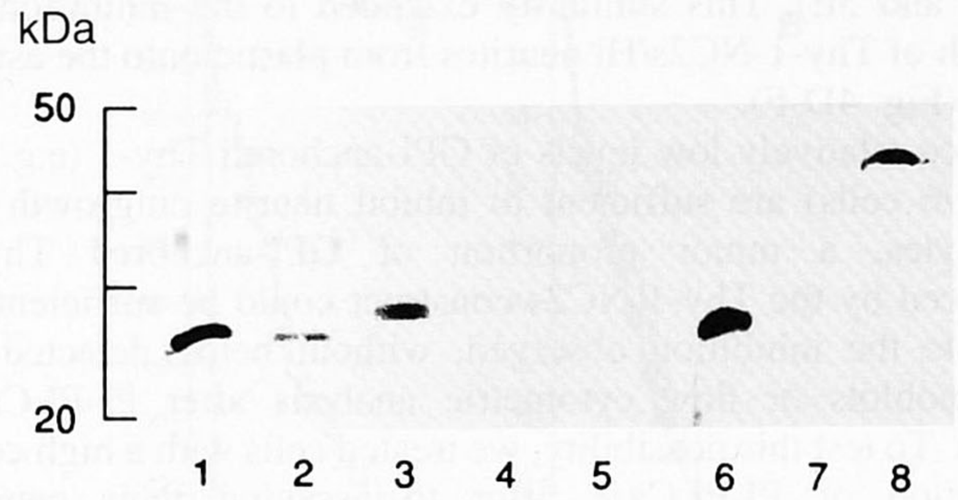

Fig. 2. Immunoblot analysis of Thy-1 on transfected cells. Lanes 1, Thy-1/3; 2, Thy-1/3 diluted 1:20; 3, Thy-1-NC2s/1; 4, Thy-1-NCms cells; 5, 20× concentrated Thy-1-NCms supernatant; 6, mouse brain membranes; 7, NG115/401L; and 8, Thy-1-NCAM-3. Protein loaded was 80-100 μg/well, except for lanes 2, 6 (20 μg) and 5 (150 μg). Bar on left calculated from a plot of R_F vs log molecular mass for marker proteins.

not shown). No cells expressing Thy-1-NCms could be identified by flow cytometry, although several neomycin-resistant clones were isolated and shown by Northern blotting to express high levels of mRNA of the size appropriate for this construct (data not shown). No Thy-1-immunoreactive band could be detected by immunoblotting, either of these cells or of their concentrated supernatant (Fig. 2, lanes 4,5) under conditions where we could readily detect Thy-1 in a 1:20 dilution of Thy-1/3 cells (Fig. 2, lane 2).

The transmembrane forms of Thy-1 were entirely resistant to PI-PLCase treatment sufficient to remove more than 90% of Thy-1 from Thy-1/3 or /9 cells (e.g. Fig. 3). Cells expressing the different Thy-1 constructs were labelled with the panel of antibodies that detect three different epitopes on mouse Thy-1.2. This labelling was assessed by flow cytometry; no differences could be seen between cells expressing normal, and transmembrane, forms of Thy-1 (data not shown).

Neurite outgrowth over astrocytes: dependence on GPI anchor

Clones expressing the different Thy-1 constructs were tested for their ability to extend neurites over a monolayer of astrocytes. In every dish, a region (approximately 30%) was left uncovered by astrocytes, so the inherent neurite growth capacity of the cells under test could be simultaneously assessed on plastic. In all cases, at least 75% of the cells extended neurites on the plastic, and were therefore inherently capable of neurite growth. As a general screening assay, cells of all clones, in different combinations of two (distinguished by labelling with the lipophilic fluorescent dyes 1,1′-dioctadecyl-3,3,3′,3′-tetramethylindocarbocyanine perchlorate (DiI) or 3,3′-dioctadecyloxacarbocyanine perchlorate (DiO) (Honig and Hume, 1986)) were added to plates of substratum cells, and assessed for the proportion of cells extending a neurite longer than one cell diameter (20-30 μm) (Table 1). In addition, for certain clones the total neurite length of 100-200 individual cells was measured (see Figs 5, 6).

Cells expressing normal Thy-1 were strongly inhibited in their neurite outgrowth on astrocytes, whereas the Thy-1-negative parental NG115/401L cells were not (Table 1; Figs 4C,J and 5A,C,D). This difference was particularly evident at the edges of the astrocyte layer, where Thy-1-positive cells extended neurites up to, but not over, the astrocytes (Fig. 4E,F), whereas Thy-1-negative cells freely extended neurites from plastic onto the astrocytes.

Clones expressing two transmembrane variants, Thy-1-NCAM and Thy-1-CD8, grew neurites over astrocytes as though they were the parental Thy-1-negative cells (Table 1; Figs 4A,B and 5B,D). However, for clones expressing the truncated NCAM cytoplasmic domains, a partial degree of inhibition of neurite outgrowth on astrocytes became evident. With two constructs expressing similar levels of Thy-1-NC28s, one clone (/1) was clearly uninhibited, whereas the other (/10) had significantly fewer cells extending neurites than did the Thy-1-negative control cells (Table 1). This difference might reflect a variation in growth potential between clones, or a functional effect of the site of insertion of the transgene. However, with the shorter construct, Thy-1-NC2s, two clones expressing higher levels of Thy-1 (/1 and /3) were clearly partially inhibited (Table 1). These results suggested that this construct might be effective in inhibiting neurite outgrowth when present at high enough density on the cell surface. We decided to test this with non-cloned populations, to average out

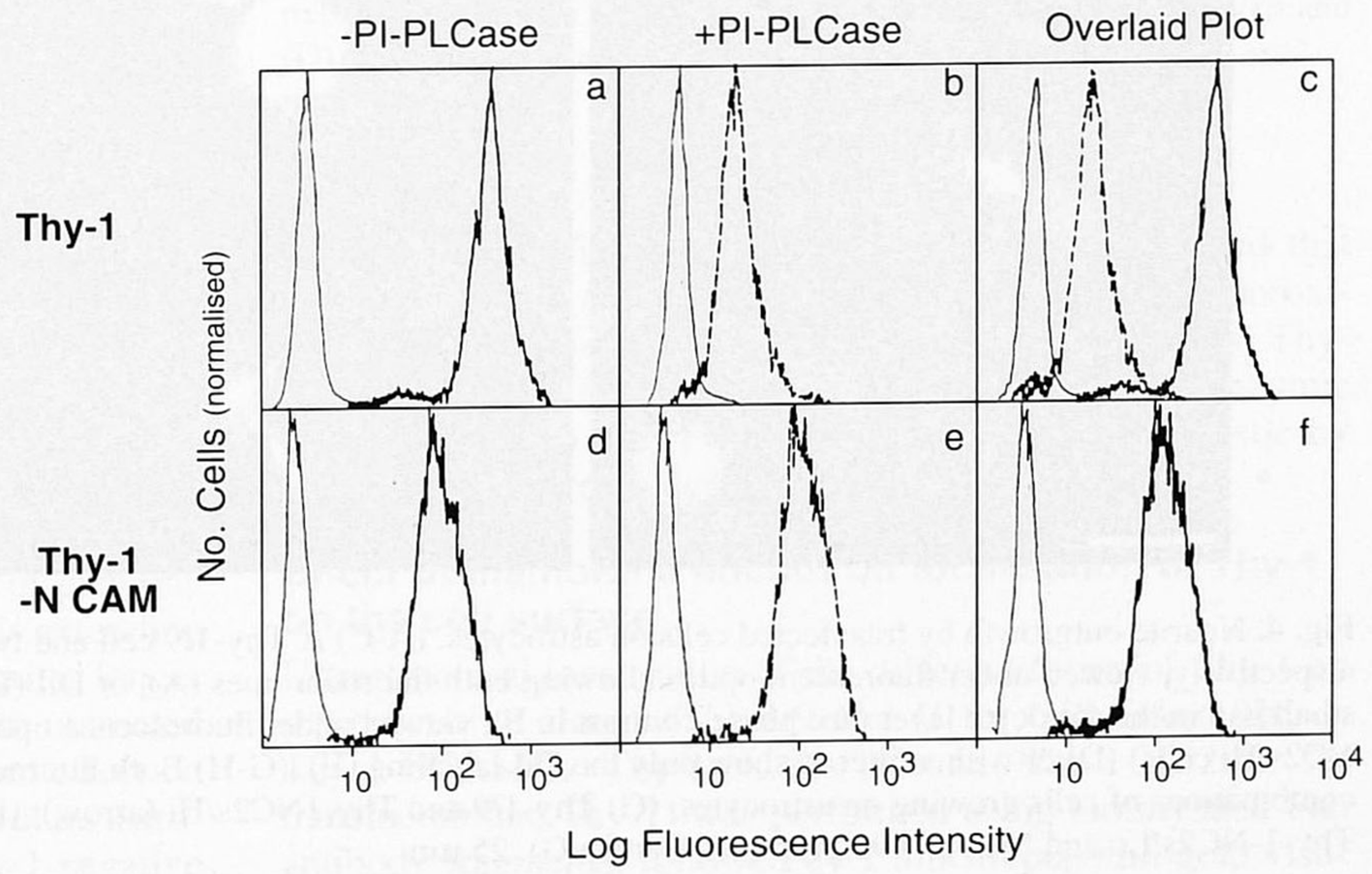

Fig. 3. Flow cytometric analysis of cells, expressing normal (GPI-anchored) Thy-1 (Thy-1/3 cells, top panel) or transmembrane Thy-1 (Thy-1-NCAM/5 cells, lower panel) immunolabelled for Thy-1, without PI-PLCase treatment (a,d), or with it (b,e), or with both plots overlaid on the same graph (c,f). In each, the profile on the left (thin line) is that obtained with cells labelled with secondary antibody only; profiles of cells labelled with H129-93.9 anti-Thy-1 antibody are the bold continuous (no PI-PLCase treatment, a,c,d,f) or broken (PI-PLCase treated, b,c,e,f) lines.

interclonal variations in neurite outgrowth potential and site-of-insertion effects. A further transfection of NG115/401L cells was done with this construct, and neomycin-resistant cells separated by flow cytometry, without cloning, into high-expressing (most intensely immunolabelled 5% of the population, called Thy-1-NC2s/Hi), and low expressing (the lowest 5-15% of the population, called Thy-1-NC2s/Lo) cells. These had, respectively, 110% and 30% of the Thy-1/9 level of surface Thy-1. The low expressing cells were mildly inhibited in their neurite outgrowth over astrocytes (Table 1; Figs 4H,J and 5F), whereas the high expressing population were as inhibited as the cells expressing normal Thy-1 (Table 1; Figs 4D-H and 5E). This similarity extended to the inhibition of growth of Thy-1-NC2s/Hi neurites from plastic onto the astrocytes (Fig. 4D-F).

Since relatively low levels of GPI-anchored Thy-1 (e.g. on Thy-1/6 cells) are sufficient to inhibit neurite outgrowth on astrocytes, a minor proportion of GPI-anchored Thy-1 produced by the Thy-1-NC2s construct could be sufficient to mediate the inhibition observed, without being detected in immunoblots or flow cytometric analysis after PI-PLCase action. To test this possibility, we treated cells with a high concentration of PI-PLCase prior to assaying their neurite outgrowth. Thy-1/3 cells, expressing high levels of normal

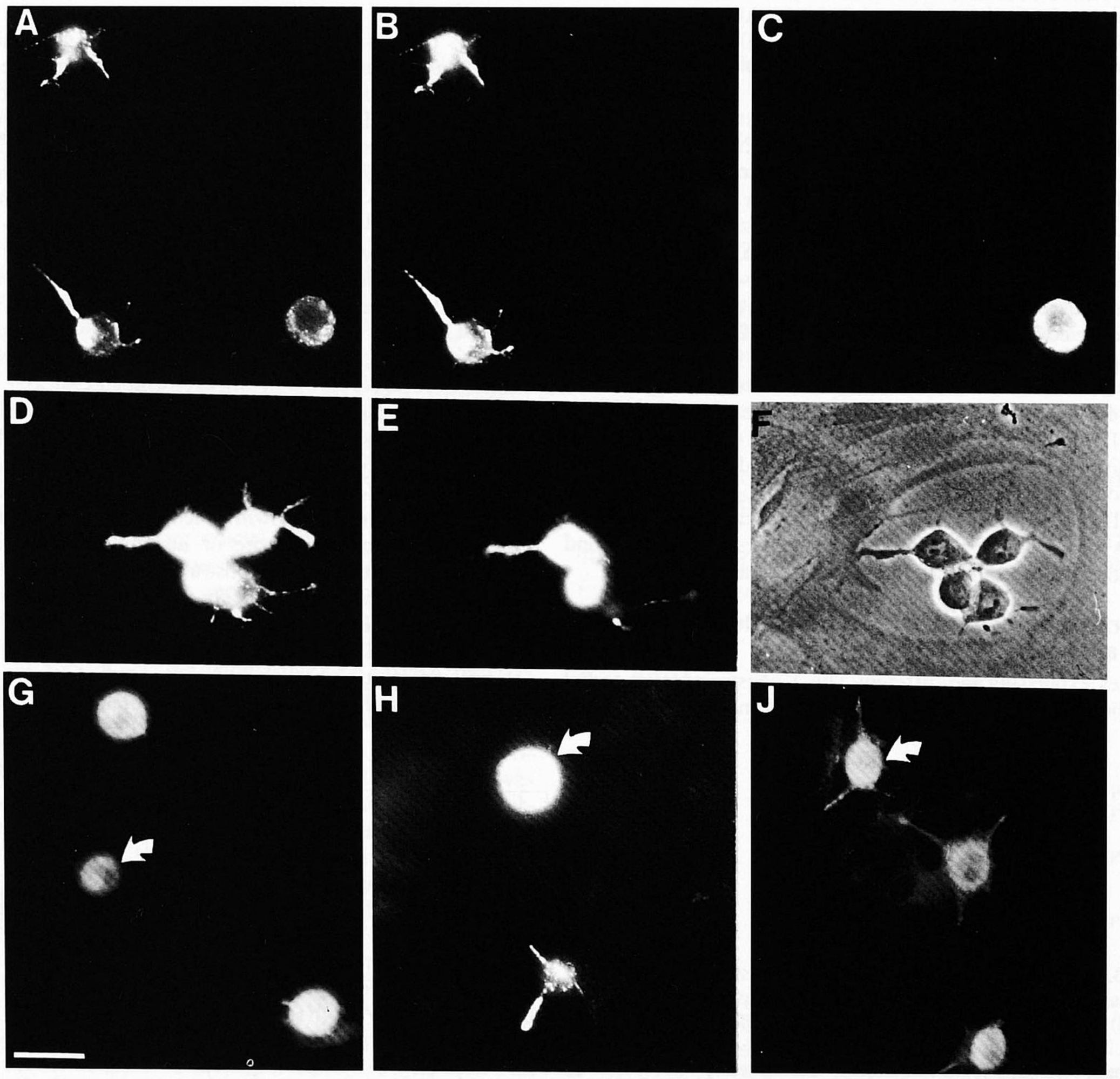

Fig. 4. Neurite outgrowth by transfected cells on astrocytes. (A-C) A Thy-1/9 cell and two Thy-1-NCAM/3 cells, labelled with DiO and DiI, respectively, viewed under fluorescent optics allowing both fluorochromes (A), or DiI (B) or DiO (C) fluorescence to be seen. (D-F) Cells in a small gap in the astrocyte layer (see phase-contrast in F), viewed under fluorescence optics to show both DiI (Thy-1/9 cells) and DiO (Thy-1-NC2s/Hi cells) (D) or with a filter to show only the DiI labelling (E). (G-H) Both fluorochromes in the same photograph, for the following combinations of cells growing on astrocytes: (G) Thy-1/9 and Thy-1NC2s/Hi (arrow); (H) Thy-1-NC2s/Hi (arrow) and Thy-1-NC2s/Lo; (J) Thy-1-NC2s/Lo and NG115/401L (arrow). Bar (in G), 25 μm.

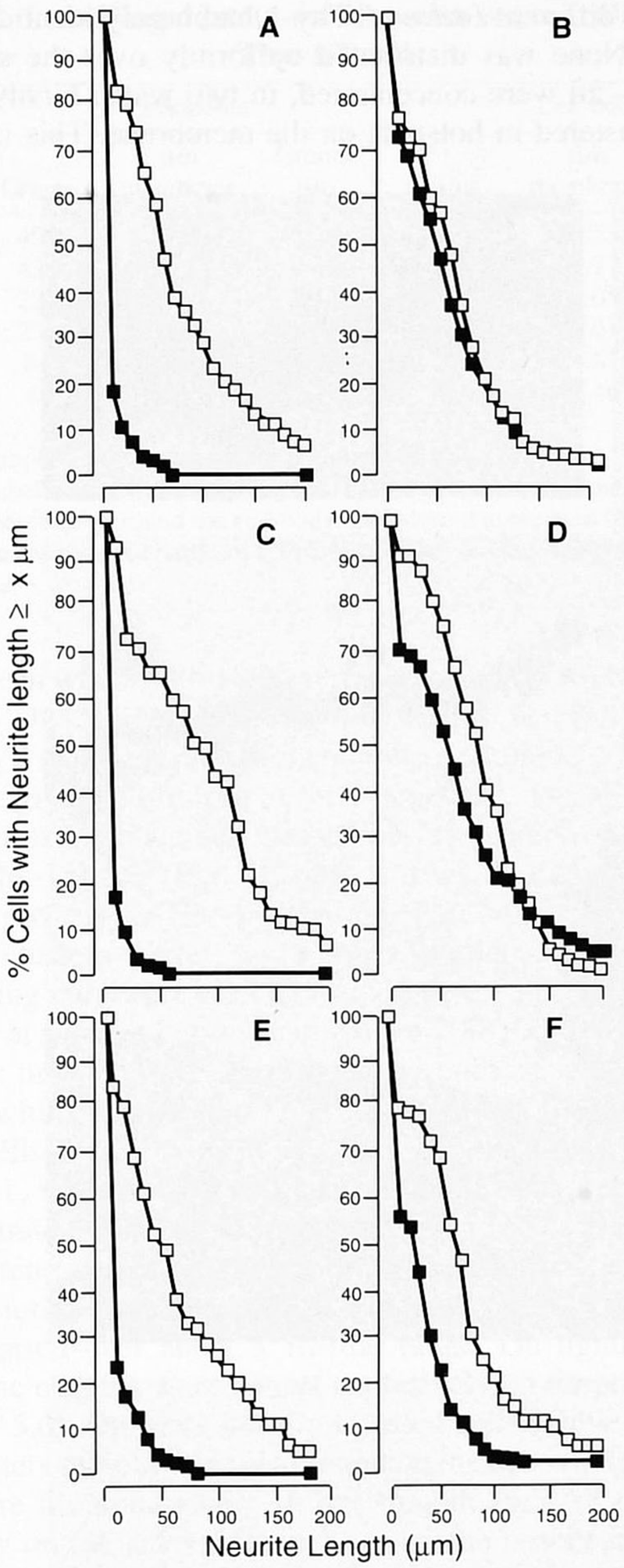

Fig. 5. Length of neurite outgrowth per cell from (A) Thy-1/3, (B) Thy-1-NCAM/3, (C) Thy-1/6, (D) NG115/401L, (E) Thy-1-NC2s/Hi, and (F) Thy-1-NC2s/Lo cells, grown for 8 hours on astrocytes (■) or on plastic areas (□) of the same dish. The percentage of cells whose total neurite length exceeds the values indicated on the *x* axis is shown.

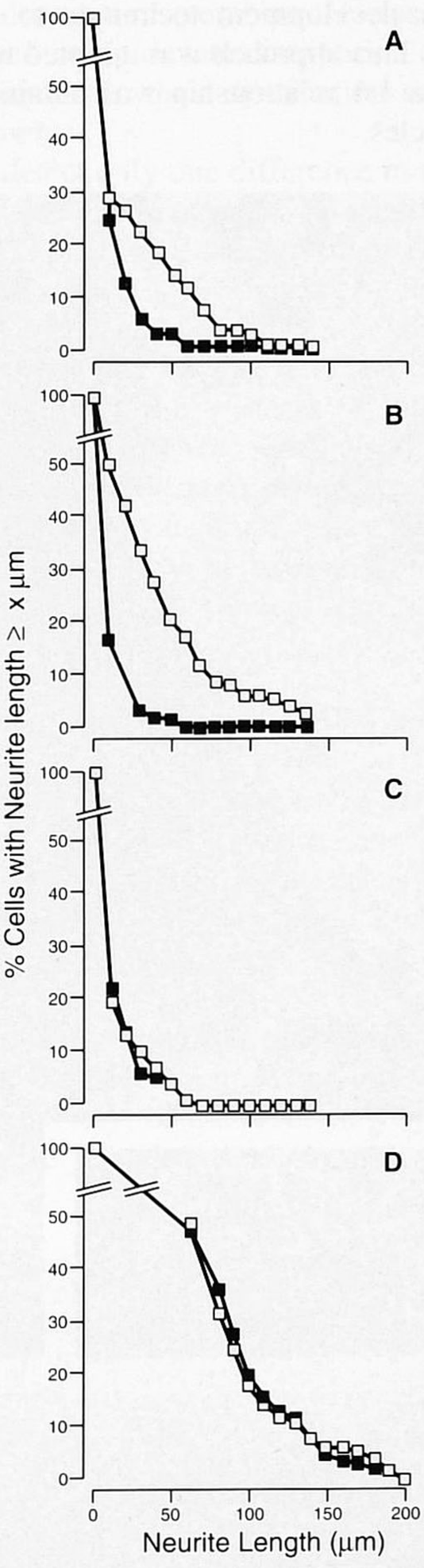

Fig. 6. Effect of PI-PLCase treatment on length of neurite outgrowth over astrocytes by (A) Thy-1/3, (B) Thy-1/6, (C) Thy-1-NC2s/Hi and (D) NG115/401L cells, without (■) or with (□) prior PI-PLCase treatment.

Thy-1, showed a mild improvement in neurite outgrowth over astrocytes as a result of PI-PLCase treatment (Fig. 6A): the proportion of cells extending a neurite increased only marginally, but the length of neurite extended by this population increased threefold. For Thy-1/6 cells, which express lower levels of normal GPI-anchored Thy-1, the effect of enzymic treatment was more marked: the proportion of cells extending a neurite trebled, and 18% of the cells extended neurites longer than 50 µm (Fig. 6B), a length never achieved with untreated cells (Figs 6B and 5C). PI-PLCase treatment had no effect on either the NC2s/Hi cells, for which neurite outgrowth on astrocytes remained inhibited (Fig. 6C), or on the Thy-1-negative NG115/401L cells. Flow cytometric analysis confirmed that the Thy-1/3 and /6 cells used in this assay had lost approximately 90% of their Thy-1, whereas there was no loss of Thy-1 from the Thy-1-NC2s/Hi cells (data not shown). Enzymic treatment had no effect on neurite outgrowth over plastic by any of the cell types (data not shown).

Effect of membrane anchor on localisation of Thy-1 on the cell surface

Ultrastructural localisation of the different forms of Thy-1 on representative clones (Thy-1/9 and /3 for GPI-linked Thy-1; Thy-1-NCAM/1, Thy-1-NC28s/10 and Thy-1-NC2s/3 for transmembrane Thy-1) was performed using biotinylated Fab antibody fragments, followed by 1 nm streptavidin-gold visu-

alised using a silver development technique to enlarge the particles to 5-25 nm. This approach was adopted to ensure, as far as possible, that a 1:1 relationship was obtained between Thy-1 and gold particles.

The four different forms of Thy-1 had nearly identical distributions. None was distributed uniformly over the surface membrane - all were concentrated, in two ways. Firstly, they were all clustered in hotspots on the membrane. This is most

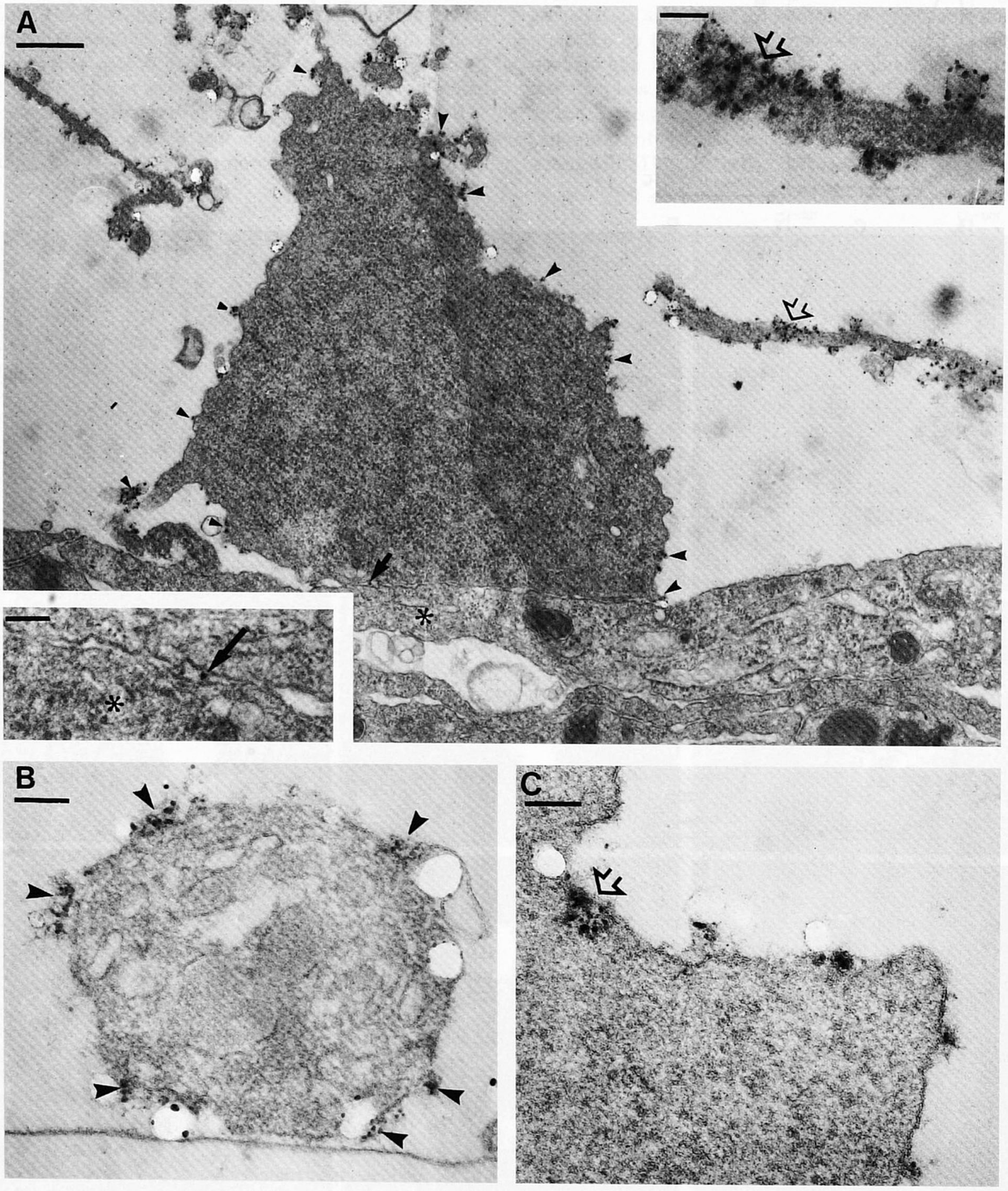

Fig. 7. Colloidal gold immunolabelling (1 nm, enhanced with silver) of Thy-1 on cells expressing Thy-1 with NCAM-140 transmembrane and cytoplasmic domains (A,B; Thy-1-NCAM/1 cells) or with the normal GPI anchor (C; Thy-1/3 cells). (A) A foot-like process (arrowheads point to some of the clusters of gold labelling) on an astrocyte (asterisk). To its right a heavily labelled filopodium, extending towards the astrocyte, is sectioned in a glancing blow that captures en face a cluster of gold labelling (open arrow, shown at higher magnification in the inset, top right). The junction formed by the foot on the astrocyte is shown at higher power in the bottom left inset (arrow points to gold label). (B) A cross-section of a filopodium (on plastic beside an astrocyte) that has several clusters of gold labelling (arrowheads). The retraction of the resin in places from around the silver-enhanced gold is a technical artefact. (C) Labelling of GPI-linked Thy-1 to be also clustered; the open arrow indicates a cluster of a dozen gold particles in a part of the membrane caught en face. Bars: 500 nm (A, main photo) and 100 nm (both insets in A; B,C).

Table 2. Labelling density on filopodia versus cell body for Thy-1/3 cells

	Filopodia			Cell body		
Cell no.	Grains	µm membrane	Grains/ µm	Grains	µm membrane	Grains/ µm
1	407	49.86	8.16	69	57.53	1.20
2	424	50.13	8.46	109	40.77	2.67
3	228	26.98	8.45	110	48.05	2.29
4	278	55.67	4.99	116	60.01	1.93
5	81	16.26	4.98	10	37.67	0.26
6	48	17.46	2.75	9	43.46	0.21

Photographs covering the entire perimeter of Thy-1/3 cells, immunolabelled with 10 nm gold particles, were analysed for their length of surface membrane around the cell body, and around associated filopodia, and for the number of gold particles (Grains) associated with each type of membrane.

easily seen where a filopodium was transected - several clusters for the Thy-1-NCAM/1 clone are visible in Fig. 7B. Occasionally a glancing slice of membrane containing a cluster was present, giving a glimpse of their large size. This is shown for a region of the main cell surface beside a filopodial extrusion for a Thy-1/9 cell (Fig. 7C open arrow), and along a fine filipodial process for Thy-1-NCAM/1 (Fig. 7A, upper inset). The larger clusters were 10-15 gold particles across, which (assuming they were circular) would give 75-175 particles per cluster, at a density of one particle per 200-1000 nm^2. No cytoplasmic or membrane specialisation could be identified associated with these clusters (nor could we identify caveolae on these cells).

Thy-1, whether GPI or transmembrane anchored, was also concentrated by being located predominantly on fine filipodia. The extent of this concentration depended upon the level of expression on individual cells, which on these clonal populations varied over about a 10-fold range. On lightly labelled cells, the clusters were almost exclusively on filopodia (Table 2, cells 5,6). On more heavily labelled cells (Table 2, cells 1-4), clusters of gold were also found on the cell surface adjacent to where filopodia emerged, but smooth areas of the surface (usually on the side of the cell, or on the basal surface away from the area of astrocyte contact) contained very few gold particles (about 0.1 grain/µm of membrane). On neurites extended by Thy-1-NCAM/1 and Thy-1-NC28s/10 clones over astrocytes, clusters of gold label were heavily concentrated on the leading edge of the neurite (not shown).

All cells had an extended area of close contact with the astrocytes, with a 10-20 nm gap between the surfaces of the two cell types (Fig. 7A, lower inset). Although the surface of the neural cell at the edge of this contact was usually well labelled, and fine filopodia extending towards the astrocytes were invariably heavily labelled (Fig. 7A), gold particles were only occasionally found in the gap between the neural cell and the astrocyte where the gap widened (e.g. Fig. 7A, lower inset). However, when fixed cells, permeabilised with either Triton X-100 or saponin before immunolabelling, were compared in the confocal microscope with cells whose membranes were intact during the application of antibodies, it was clear that the lack of labelling was due to the failure of the antibodies to penetrate to Thy-1 in the area of contact. On permeabilised cells, no differences could be seen between GPI-anchored and transmembrane forms of Thy-1, both of which occurred in a punctate distribution on the basal surface of the cell, similar to their distribution on the upper surface (data not shown).

We could detect only one difference in the surface distribution of the transmembrane and GPI-anchored forms of Thy-1 on these cells expressing a single form of Thy-1: with the transmembrane- but not GPI-anchored forms, immunogold labelling was consistently found in a small proportion (1-10%) of the coated pits (Fig. 8). The label was always near the rim of the pit, possibly because access of antibody to the deeper regions was prevented. (Note that the cells were fixed before labelling, and could not internalise the gold.) For each transmembrane form of Thy-1, immunolabel was encountered in a coated pit with every few cells inspected, but was not found there in over a thousand cells that were examined expressing GPI-anchored Thy-1.

Double labelling of GPI-anchored and transmembrane Thy-1

To test more stringently whether the microdomains on the surface membrane occupied by the GPI- and transmembrane-anchored forms of Thy-1 are identical or mutually exclusive, we immunolabelled the two forms on doubly transfected cells expressing transmembrane mouse Thy-1 (Thy-1-NCAM and Thy-1-NC2s) and normal (GPI-linked) human Thy-1. Co-expressing cells, selected by flow cytometry, had levels of GPI-anchored, and transmembrane, Thy-1 that were 60-80% and 20-30%, respectively, of the level on Thy-1/9 cells. Cells on astrocytes were labelled for electron microscopy, using

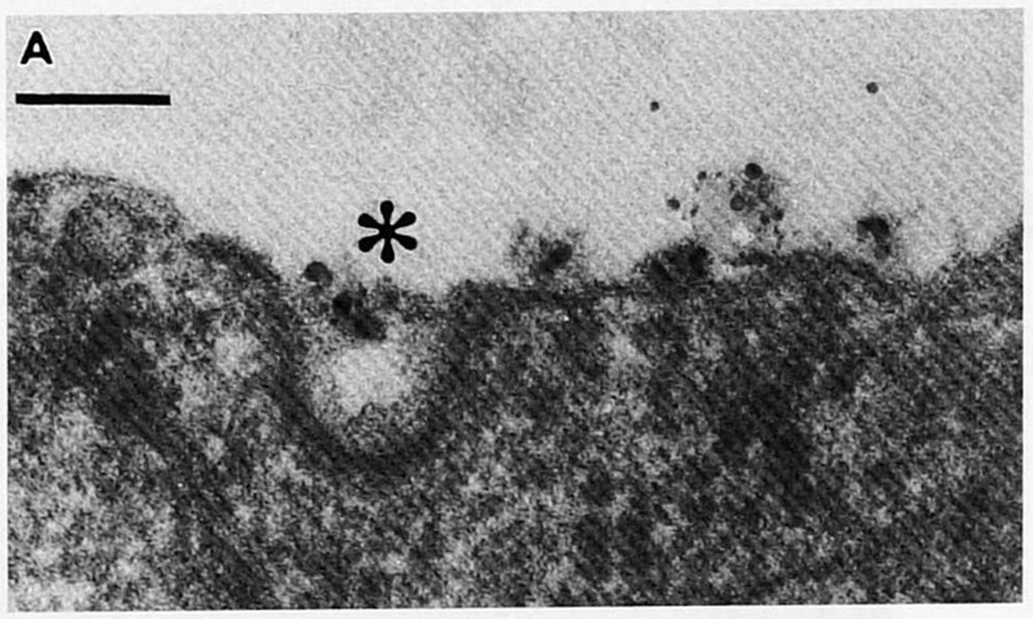

Fig. 8. Silver-enhanced immunogold labelling for Thy-1-NCAM within coated pits (below large asterisks): Thy-1-NCAM/1 cells. Bars, 100 nm.

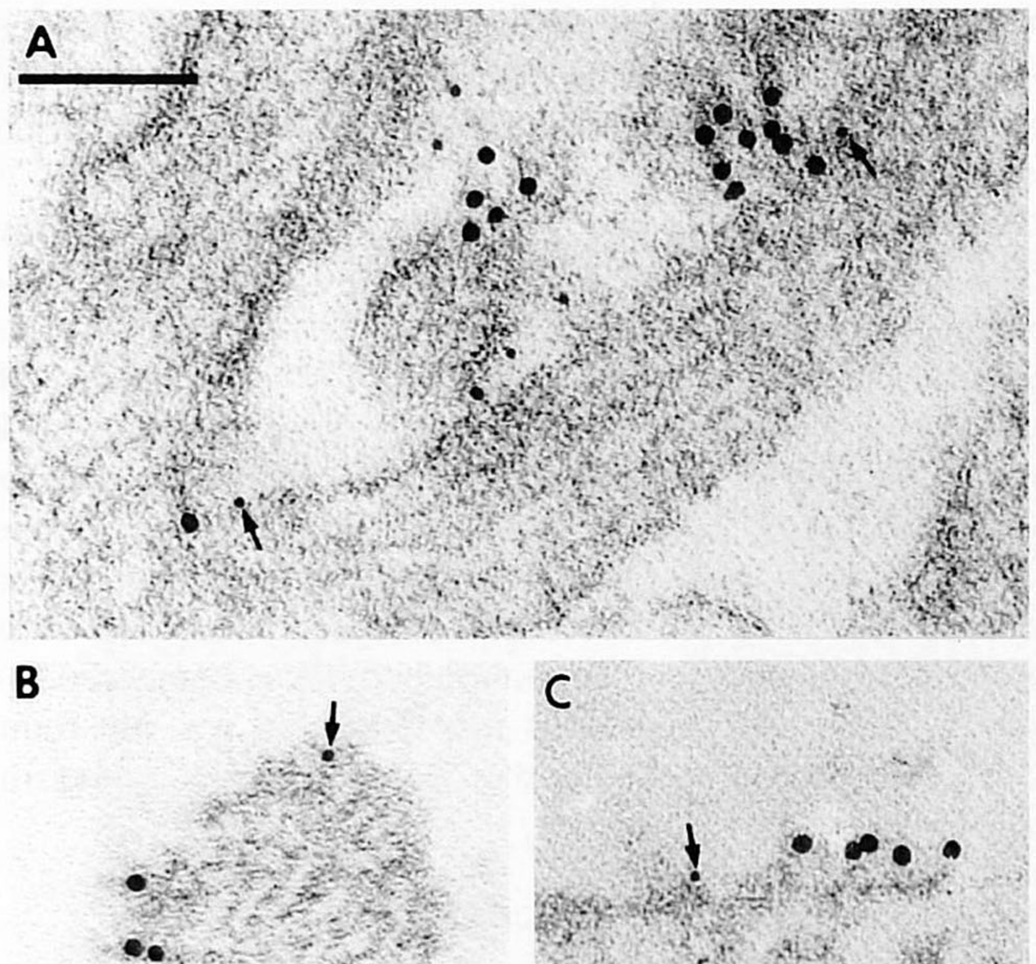

Fig. 9. Dual labelling for GPI-anchored human Thy-1 (10 nm gold) and transmembrane mouse Thy-1 (A-C: Thy-1-NCAM; D-E: Thy-1-NC2s, both labelled with 5 nm gold, some of which are indicated by arrows). Bars, 100 nm (B,C same magnification as A; E-G same as D).

primary antibodies that were specific for mouse and human Thy-1, with 10 nm gold to identify GPI-anchored Thy-1 and 5 nm gold for the transmembrane form. The distribution already described (clustered labelling, predominantly of filopodia) was again apparent for each construct.

For Thy-1-NCAM and human Thy-1 cotransfectants, the clusters of each form of Thy-1 were always separate. Fig. 9 A-C shows examples of a 5 nm gold particle (i.e. Thy-1-NCAM) occurring in close proximity to one or a cluster of 10 nm gold particles (GPI-anchored Thy-1). In Fig. 9A there are two prominent clusters (seen en face) of 10 nm gold particles that lie on the surface of a filopodium cut in a glancing blow. Below this is a longitudinal section of another filopodia, on which there are two examples (arrows) of a 5 nm particle that lies within 50 nm of a 10 nm particle. These were the closest examples found from several hundred cells surveyed; Fig. 9B,C shows cases where a 5 nm particle lies within 100 nm of a cluster of 10 nm particles. Even these cases were relatively rare, and a few hundred nm usually separated clusters of the two forms of Thy-1.

With the human Thy-1 and Thy-1-NC2s cotransfectants, separate clusters of each form were also seen, but in addition approximately 10% of the 5 nm grains were found within the clusters of 10 nm particles. The smaller grains were most commonly found at the edge of a 10 nm cluster (e.g. Fig. 9E,G), but instances where the smaller particle was found within the cluster also occurred (e.g. Fig. 9D,F).

To complement this analysis in the electron microscope, we examined doubly transfected cells in the confocal microscope, whose level of resolution (approaching 200 nm; Brakenhoff et al., 1979) should be sufficient to separate many of the clusters of label. We analysed cells expressing higher levels of transmembrane Thy-1, with approximately equivalent levels of GPI-anchored Thy-1. A 1 μm optical section was taken through the centre of such cells, and the localisation of each form determined by overlaying the image obtained with the filters for FITC (labelling transmembrane Thy-1) and Texas Red (labelling GPI Thy-1). Typical results are shown in Fig. 10. In cells expressing human (GPI) Thy-1 and Thy-1-NCAM (e.g. see Fig. 10A), regions that were purely labelled for one or other form, seen as red or green, respectively, could readily be found on every cell examined. In addition, yellow/orange regions labelled for both forms also occurred, presumably indicating membrane where less than 200 nm separated the clusters of the two forms of Thy-1. A similar separation of the label for the transmembrane and GPI forms was evident in co-transfectants expressing human Thy-1 and Thy-1-CD8 (not shown). In contrast, on cells expressing Thy-1-NC2s and normal Thy-1, regions that were purely labelled for the transmembrane form were infreqently found - most of the green label occurred with the red label (e.g. Fig. 10B). On cells expressing human and mouse GPI-anchored Thy-1, the label for the two forms showed identical distributions on the surface (not shown). Thus, in the confocal microscope also, Thy-1-NC2s was found to have a close, although not identical, association with GPI-anchored Thy-1, whereas the clusters of Thy-1-NCAM or Thy-1-CD8 were distinct from those of normal Thy-1.

DISCUSSION

To test the hypothesis that the GPI group directs the proteins that it anchors to spatially and functionally discrete microdomains on the surface membrane, we have compared native, GPI-anchored Thy-1 to that of different transmembrane forms. We made Thy-1-CD8 as a transmembrane form in which the polypeptide sequence that substitutes for the GPI anchor is, as far as is known, functionally neutral. We also based a series of constructs on the transmembrane and cytoplasmic domains of NCAM-140, anticipating that the NCAM domains might confer additional functional properties, or cellular localization signals, that could be informative.

The conformation of the Thy-1 domain in the hybrid proteins was initially assessed with a panel of monoclonal antibodies that recognize three separate epitopes on Thy-1 (Pont et al., 1985). The hybrid proteins reacted as though they were native Thy-1. More direct evidence for the integrity of the

extracellular domain of Thy-1 in the transmembrane proteins emerged from their behaviour in functional assays. One transmembrane form, Thy-1-NC2s, has an active Thy-1 domain, since it inhibited neurite outgrowth over astrocytes. Structurally, the extracellular domains of Thy-1-NC2s do not differ significantly from those of the other transmembrane constructs;

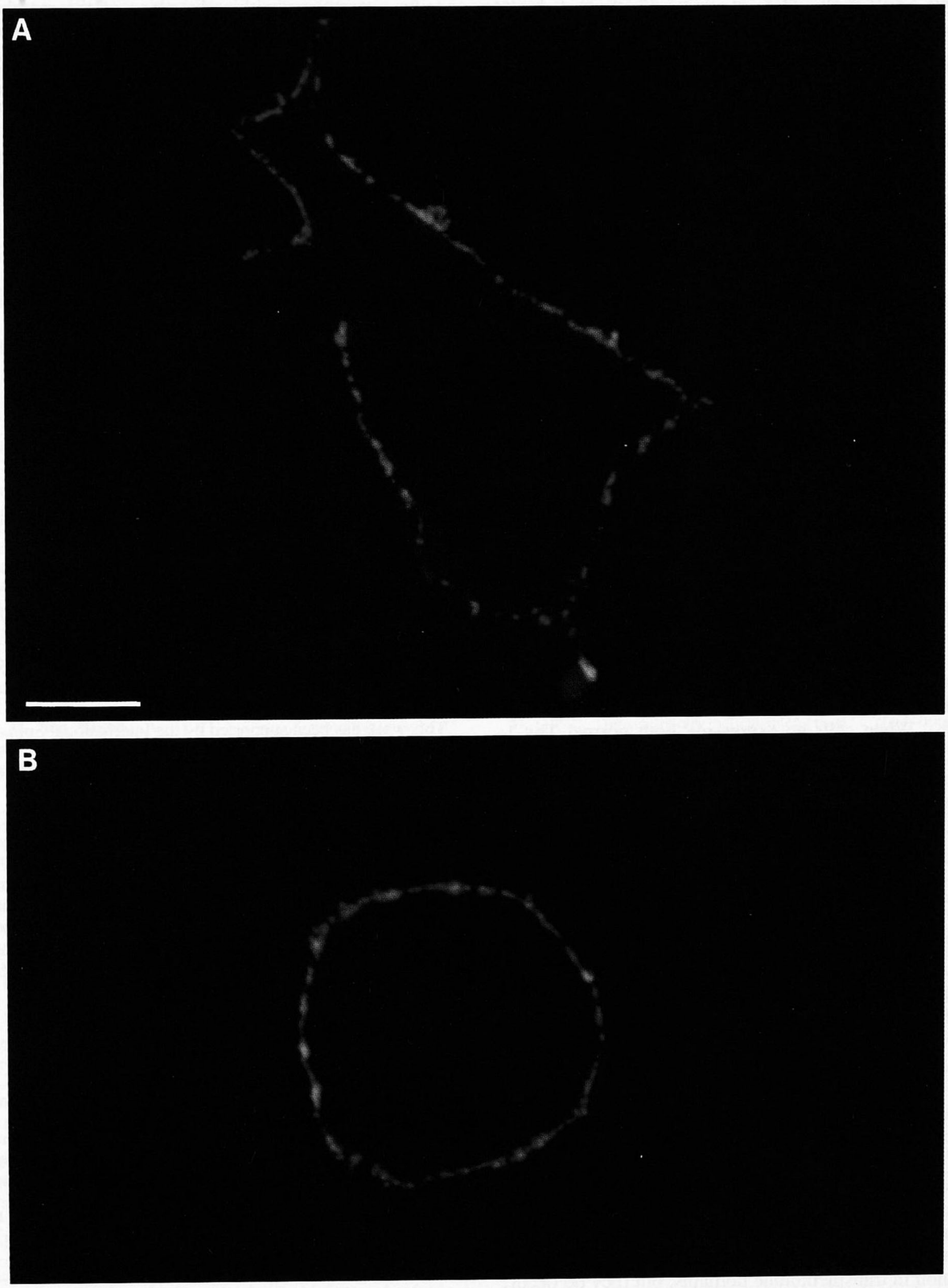

Fig. 10. Confocal images (1 μm section) of double labelling for human (GPI-anchored) Thy-1 (seen with Texas Red fluorescence) and either Thy-1-NCAM (A) or Thy-1-NC2s (B; both transmembrane forms seen with green FITC fluorescence). Bar, 10 μm.

the inability of the latter to inhibit neurite outgrowth must therefore arise from differences within the membrane or cytoplasmic domains.

The functional difference between the GPI and transmembrane forms of Thy-1 is not due to their being localised to different parts of the cell: all forms were clustered at high density in patches on the membrane, located predominantly on filopodia. Here they are ideally placed to control neurite outgrowth, since these fine extensions provide the foci for growth cone extension (Davenport et al., 1993). This undoubtedly explains the very high efficiency of native Thy-1's inhibitory action on these cells. We were unable, with the transfected cells used here, to define the lower limits of Thy-1 expression that would fail to inhibit neurite outgrowth on astrocytes. Thy-1/9 and /6 cells differ 20-fold in their level of Thy-1 (being approximately equivalent to that of high- and low-Thy-1-expressing neurons in vivo; Morris and Grosveld, 1989), yet the neurite outgrowth of both was fully inhibited. However, when PI-PLCase reduced the level of surface Thy-1 on the lower expressing cells to about 0.5% the Thy-1/9 level, partial inhibition of outgrowth was obtained.

This partial inhibition seen with PI-PLCase-treated Thy-1/6 cells was comparable to that seen with cells expressing approximately a 100-fold higher level of Thy-1-NC2s (e.g. /1, /3 and /Lo cells; Table 1 and Fig. 5F, compared to Fig. 6B). Thy-1-NC2s, therefore, is approximately 1% as efficient as GPI-anchored Thy-1 in inhibiting neurite outgrowth.

The GPI anchor determines the precise microdomain occupied by Thy-1 on the membrane. Neither form was seen to be associated with a membrane structure such as caveolae (although the major protein of caveolae, caveolin, is not expressed in brain; Glenney, 1989). However, GPI-Thy-1, but not any of the transmembrane forms, was excluded from coated pits (also observed with other GPI-anchored glycoproteins; e.g. Bamezai et al., 1992; Keller et al., 1992; Rothberg et al., 1990b). When cells co-expressing both normal Thy-1 and Thy-1-NCAM were analysed, no overlap at all was found between the clusters of GPI-, and transmembrane-anchored, Thy-1. Thus the two forms occupy separate microdomains on the surface, and their access to other molecules required to complete a receptor unit (including a transmembrane signalling molecule) could be quite different. Evidence suggesting that this is so came from the analysis of cells co-expressing normal Thy-1 and Thy-1-NC2s, the transmembrane form that inefficiently inhibits neurite outgrowth. Although most Thy-1-NC2s occurred in clusters different from those containing GPI-anchored Thy-1, approximately 10% of the label for the transmembrane form occurred within the clusters of normal Thy-1. At high levels of expression of Thy-1-NC2s, this partial penetration could allow functional concentrations of transmembrane Thy-1 to build up within the GPI microenvironment. Thus inclusion of Thy-1 in the GPI microdomains appears to be the critical factor determining whether it can inhibit neurite outgrowth on astrocytes; conversely, the GPI anchor itself would not appear to be directly required for Thy-1 function.

The ability of Thy-1-NC2s to partly penetrate the GPI domains on the membrane is probably due to the Asp residue buried within its transmembrane segment. Charged residues are uncommon in transmembrane domains, but they do occur; for instance, in molecules that associate with the T cell receptor complex where they interact with buried basic residues on other polypeptide components to establish multimeric complexes (Manolios et al., 1990; Rutledge et al., 1992). The buried Asp residue within the transmembrane domain of NCAM (and its *Drosophila* homologue, fasciclin II; Harrelson and Goodman, 1988) is potentially an active centre, directing specific interactions within the plane of the membrane with other proteins containing a transmembrane Lys or Arg residue. Should a protein with a positively charged residue buried at the appropriate level in the membrane occur within the GPI domains, Thy-1-NC2s could bind to it and so partition into the GPI domains. Such ectopic charge-pair formation has been demonstrated for mutant transmembrane domains into which an Asp residue has been introduced (Lankford et al., 1993). The other NCAM-based transmembrane forms have part or all of the NCAM-140 cytoplasmic domain that must impart additional constraints to impede their entry into the GPI domains.

How the GPI anchor determines the microdomain occupied by a protein, how Thy-1 mediates an inhibition of neurite outgrowth, and whether this mechanism is found with real neurons (as distinct from a cell line), remain subjects for further study. Although the NG115/401L cells have been invaluable for functional studies, they have proved unsuitable for molecular analysis. We have found it impossible, for instance, to define a specific Thy-1 immunoprecipitate from detergent lysates of these cells, due to non-specific immunoprecipitation. We have expressed GPI-linked Thy-1 and Thy-1-NCAM in another neural cell line (ND22) and find that a protein kinase activity co-immunoprecipitates from a Brij 96 cell lysate with the normal, but not transmembrane-linked, Thy-1 (unpublished observations). This illustates the potential to move the analysis of these constructs to a more molecular level, for which we are developing transgenic mice to allow us to carry out concerted functional, molecular and cytoarchitectural studies.

This work has been supported by the International Spinal Research Trust, American Paralysis Association, International Institute for Research in Paraplegia, Royal Society, Wellcome Trust, CNRS and the MRC. We thank Chris Atkins for his assistance with flow cytometry and sorting; David Jones for analysing the NCAM transmembrane domain; Hai Tao He, Michel Pierres and Mary Ritter for providing hybridoma lines; Colin Young for their bulk protein-free culture; Ann Leach for mycoplasma surveillance; Ian Burdett, Peter Bailey and Jean Lawrence for assistance with confocal and electron microscopy; Rose Zamoyska for pLy-2a′.RVxpUC; the late Richard Akeson for pRB7; Niels Galjart and David Michaelovitch for useful discussions; and Andy Furley, Christo Goridis and Geof Raisman for their comments on the manuscript.

REFERENCES

Anderson, R. G. W. (1993). Caveolae: where incoming and outgoing messengers meet. *Proc. Nat. Acad. Sci. USA* **90**, 10909-13.

Bamezai, A., Goldmacher, V. S. and Rock, K. L. (1992). Internalization of glycosyl-phosphatidylinositol (GPI)-anchored lymphocyte proteins. II. GPI-anchored and transmembrane molecules internalize through distinct pathways. *Eur. J. Immunol.* **22**, 15-21.

Barclay, A. N., Birkeland, M. L., Brown, M. H., Beyers, A. D., Davis, S. J., Somoza, C. and Williams, A. F. (1993). *The Leucocyte Antigen Facts Book.* London: Academic Press.

Brakenhoff, G. J., Blom, P. and Barends, P. (1979). Confocal scanning light microscopy with high aperture lenses. *J. Microsc.* **117**, 219-232.

Brown, D. A. (1992). Interactions between GPI-anchored proteins and membrane lipids. *Trends Cell Biol.* **2**, 338-343.

Burry, R. W., Vandre, D. D. and Hayes, D. M. (1992). Silver enhancement of gold antibody probes in pre-embedding electron microscopic immunohistochemistry. *J. Histochem. Cytochem.* **1992**, 1849-1856.

Cramer, W. A., Engelman, D. M., Heijne, G. v. and Rees, D. C. (1992). Forces involved in the assembly and stabilization of membrane proteins. *FASEB J.* **6**, 3397-402.

Cunningham, B. A., Hemperly, J. J., Murray, B. A., Prediger, E. A., Brackenbury, R. and Edelman, G. M. (1987). Neural cell adhesion molecule: structure, immunoglobulin-like domains, cell surface modulation, and alternative RNA splicing. *Science* **236**, 799-806.

Davenport, R. W., Dou, P., Rehder, V. and Kater, S. B. (1993). A sensory role for neuronal growth cone filopodia. *Nature* **361**, 721-723.

Dickson, G., Gower, H. J., Barton, C. H., Prentice, H. M., Elsom, V. L., Moore, S. E., Cox, R. D., Quinn, C., Putt, W. and Walsh, F. S. (1987). Human muscle neural cell adhesion molecule (N-CAM): identification of a muscle-specific sequence in the extracellular domain. *Cell* **50**, 1119-1130.

Doherty, P. and Walsh, F. S. (1992). Cell adhesion molecules, second messengers and axonal growth. *Curr. Opin. Neurobiol.* **2**, 595-601.

Dustin, M. L. and Springer, T. A. (1991). Role of lymphocyte adhesion receptors in transient interactions and cell locomotion. *Annu. Rev. Immunol.* **9**, 27-66.

Ferguson, M. A. J. (1992). Glycosyl-phosphatidylinositol membrane anchors: The tale of a tail. *Biochem. Soc. Trans.* **20**, 243-256.

Fujimoto, T. (1993). Calcium pump of the plasma membrane is localized in caveolae. *J. Cell Biol.* **120**, 1147-1157.

Fujimoto, T., Nakade, S., Miyawaki, A., Mikoshiba, K. and Ogawa, K. (1993). Localization of inositol 1,4,5,-triphosphate receptor-like protein in plasmalemmal caveolae. *J. Cell Biol.* **119**, 1507-1513.

Glenney, J. R. (1989). Tyrosine phosphorylation of a 22-kDa protein is correlated with transformation by Rous sarcoma virus. *J. Biol. Chem.* **264**, 20163-6.

Harrelson, A. L. and Goodman, C. S. (1988). Growth cone guidance in insects: fasciclin II is a member of the immunoglobulin superfamily. *Science* **242**, 700-708.

Homans, S. W., Ferguson, M. A., Dwek, R. A., Rademacher, T. W., Anand, R. and Williams, A. F. (1988). Complete structure of the glycosyl phosphatidylinositol membrane anchor of rat brain Thy-1 glycoprotein. *Nature* **333**, 269-72.

Honig, M. G. and Hume, R. I. (1986). Fluorescent carbocyanine dyes allow living neruons of identified origin to be studied in long-term cultures. *J. Cell Biol.* **103**, 171-187.

Hooper, N. M. and Bashir, A. (1991). Glycosyl-phosphatidylinositol-anchored membrane proteins can be distinguished from transmembrane polypeptide-anchored proteins by differential solubilization and temperature-induced phase separation in Triton X-114. *Biochem. J.* **280**, 745-751.

Hooper, N. M. (1992). More than just a membrane anchor. *Curr. Biol.* **2**, 617-619.

Jones, D. T., Taylor, W. R. and Thornton, J. M. (1994). A model recognition approach to the prediction of all-helical membrane protein structure and topology. *Biochemistry* **33**, 3038-3049.

Keller, G. A., Siegel, M. W. and Caras, I. W. (1992). Endocytosis of glycophospholipid-anchored and transmembrane forms of CD4 by different endocytic pathways. *EMBO J.* **11**, 863-874.

Laemmli, U. K. (1970). Cleavage of structural proteins during the assembly of the head of bacteriophage T4. *Nature* **277**, 680-685.

Lankford, S. P., Cosson, P., Bonifacino, J. S. and Klausner, R. D. (1993). Transmembrane domain length affects charge-mediated retention and degradation of proteins within the endoplasmic reticulum. *J. Biol. Chem.* **268**, 4814-20.

Ledbetter, J. A. and Herzenberg, L. A. (1979). Xenogeneic monoclonal antibodies to mouse lymphoid differentiation antigens. *Immunol. Rev.* **47**, 63-90.

Lisanti, M. P., Tang, Z. L. and Sargiacomo, M. (1993). Caveolin forms a hetero-oligomeric protein complex that interacts with an apical GPI-linked protein: implications for the biogenesis of caveolae. *J. Cell Biol.* **123**, 595-604.

Manolios, N., Bonifacino, J. S. and Klausner, R. D. (1990). Transmembrane helical interactions and the assembly of the T cell receptor complex. *Science* **249**, 274-7.

Miyata, T., Isobe, K., Dawson, R., Ritter, M. A., Inagi, R., Oda, O., Taguchi, R., Ikezawa, H., Inoue, I., Seo, H., Hasegawa, M., Kobayashi, S., Maeda, K., Yamada, K. and Nakashima, I. (1990). Determination of the molecular nature and cellular localization of Thy-1 in human renal tissue. *Immunology* **69**, 391-5.

Morris, R. J. and Barber, P. C. (1983). Fixation of Thy-1 in nervous tissue for immunohistochemistry: a quantitative assessment of the effect of different fixation conditions upon retention of antigenicity and the cross-linking of Thy-1. *J. Histochem. Cytochem.* **31**, 263-274.

Morris, R. J., Barber, P. C., Beech, J. and Raisman, G. (1983). The distribution of Thy-1 antigen in the P.N.S. of the adult rat. *J. Neurocytol.* **12**, 1017-1039.

Morris, R. J. and Grosveld, F. (1989). Expression of Thy-1 in the nervous system of the rat and mouse. In *Cell Surface Antigen Thy-1. Immunology, Neurology and Therapeutic Applications* (ed. A. E. Reif and M. Schlesinger), pp. 121-148. New York and Basel: Marcel Dekker, Inc.

Morris, R. (1992). Thy-1, the enigmatic extrovert on the neuronal surface. *BioEssays* **14**, 715-722.

O'Dowd, B. F., Hnarowich, M., Caron, M. G., Lefkowitz, R. J. and Bouvier, M. (1989). Palmitoylation of the human β2-adrenergic receptor. *J. Biol. Chem.* **264**, 7564-7569.

Parenti, M. and Magee, A. I. (1994). Fatty acid- and isoprenoid-linked membrane proteins. In *Biomembranes* (ed. A. G. Lee). Greenwich CT: JAI Press Inc. (in press).

Pont, S., Regnier-Vigouroux, A., Naquet, P., Blanc, D., Pierres, A., Marchetto, S. and Pierres, M. (1985). Analysis of the Thy-1 pathway of T cell hybridoma activation using 17 rat monoclonal antibodies reactive with distinct Thy-1 epitopes. *Eur. J. Immunol.* **15**, 1222-1228.

Ravetch, J. V. and Kinet, J. P. (1991). Fc receptors. *Annu. Rev. Immunol.* **9**, 457-92.

Robinson, P. J., Millrain, M., Antoniou, J., Simpson, E. and Mellor, A. L. (1989). A glycophospholipid anchor is required for Qa-2-mediated T cell activation. *Nature* **342**, 85-7.

Robinson, P. J. (1991). Phosphatidylinositol membrane anchors and T-cell activation. *Immunol. Today* **12**, 35-41.

Robson, B. and Suzuki, E. (1976). Conformational properties of amino acid residues in globular proteins. *J. Mol. Biol.* **107**, 327-356.

Rothberg, K. G., Ying, Y. S., Kamen, B. A. and Anderson, R. G. (1990a). Cholesterol controls the clustering of the glycophospholipid-anchored membrane receptor for 5-methyltetrahydrofolate. *J. Cell Biol.* **111**, 2931-8.

Rothberg, K. G., Ying, Y. S., Kolhouse, J. F., Kamen, B. A. and Anderson, R. G. (1990b). The glycophospholipid-linked folate receptor internalizes folate without entering the clathrin-coated pit endocytic pathway. *J. Cell Biol.* **110**, 637-49.

Rutledge, T., Cosson, P., Manolios, N., Bonifacino, J. S. and Klausner, R. D. (1992). Transmembrane helical interactions: ζ chain dimerization and functional association with the T cell antigen receptor. *EMBO J.* **11**, 3245-54.

Santoni, M. J., Barthels, D., Barbas, J. A., Hirsch, M. R., Steinmetz, M., Goridis, C. and Wille, W. (1987). Analysis of cDNA clones that code for the transmembrane forms of the mouse neural cell adhesion molecule (NCAM) and are generated by alternative RNA splicing. *Nucl. Acids Res.* **15**, 8621-8641.

Sargiacomo, M., Sudol, M., Tang, Z. and Lisanti, M. P. (1993). Signal transducing molecules and glycosyl-phosphatidylinositol-linked proteins form a caveolin-rich insoluble complex in MDCK cells. *J. Cell Biol.* **122**, 789-807.

Shaw, A. S., Chalupny, J., Whitney, J. A., Hammond, C., Amrein, K. E., Kavathas, P., Sefton, B. M. and Rose, J. K. (1990). Short related sequences in the cytoplasmic domains of CD4 and CD8 mediate binding to the amino-terminal domain of the $p56^{lck}$ tyrosine protein kinase. *Mol. Cell Biol.* **10**, 1853-62.

Shenoy-Scaria, A. M., Kwong, J., Fujita, T., Olszowy, M. W., Shaw, A. S. and Lublin, D. M. (1992). Signal transduction through decay-accelerating factor. Interaction of glycosyl-phosphatidylinositol anchor and protein tyrosine kinases $p56^{lck}$ and $p59^{fyn}$. *J. Immunol.* **149**, 3535-41.

Sipos, L. and Heijne, G. v. (1993). Predicting the topology of eukaryotic membrane proteins. *Eur. J. Biochem.* **213**, 1333-40.

Small, S. J., Shull, G. E., Santoni, M. J. and Akeson, R. (1987). Identification of a cDNA clone that contains the complete coding sequence for a 140-kD rat NCAM polypeptide. *J. Cell Biol.* **105**, 2335-45.

Stefanova, I., Horejsi, V., Ansotegui, I. J., Knapp, W. and Stockinger, H. (1991). GPI-anchored cell-surface molecules complexed to protein tyrosine kinases. *Science* **254**, 1016-9.

Su, B., Waneck, G. L., Flavell, R. A. and Bothwell, A. L. M. (1991). The glycosyl phosphatidylinositol anchor is critical for Ly-6A/E-mediated T cell activation. *J. Cell Biol.* **112**, 377-384.

Thomas, P. M. and Samelson, L. E. (1992). The glycophosphatidylinositol-

anchored Thy-1 molecule interacts with the p60^{fyn} protein tyrosine kinase in T cells. *J. Biol. Chem.* **267**, 12317-22.

Tiveron, M. C., Barboni, E., Pliego Rivero, F. B., Gormley, A. M., Seeley, P. J., Grosveld, F. and Morris, R. (1992). Selective inhibition of neurite outgrowth on mature astrocytes by Thy-1 glycoprotein. *Nature* **355**, 745-8.

Vidal, M., Morris, R., Grosveld, F. and Spanopoulou, E. (1990). Tissue-specific control elements of the Thy-1 gene. *EMBO J.* **9**, 833-40.

Volarevic, S., Burns, C. M., Sussman, J. J. and Ashwell, J. D. (1990). Intimate association of Thy-1 and the T-cell antigen receptor with the CD45 tyrosine phosphatase. *Proc. Nat. Acad. Sci. USA* **87**, 7085-9.

Walsh, F. S. and Doherty, P. (1992). Glycosylphosphatidylinositol-anchored recognition molecules that function in axonal fasciculation, growth and guidance in the nervous system. In *GPI Membrane Anchors* (ed. M. Lucia Cardoso de Almeida), pp. 294-309. London: Academic Press.

Williams, A. F. (1989). The structure of Thy-1 antigen. In *Cell Surface Antigen Thy-1. Immunology, Neurology and Therapeutic Applications* (ed. A. E. Reif and M. Schlesinger), pp. 49-70. New York and Basel: Marcel Dekker, Inc.

Williams, A. F., Davis, S. J., He, Q. and Barclay, A. N. (1989). Structural diversity in domains of the immunoglobulin superfamily. *Cold Spring Harb. Symp. Quant. Biol.* **2**, 637-47.

Xue, G. P. and Morris, R. (1992). Expression of the neuronal surface glycoprotein Thy-1 does not follow appearance of its mRNA in developing mouse Purkinje cells. *J. Neurochem.* **58**, 430-40.

Ying, Y. S., Anderson, R. G. and Rothberg, K. G. (1992). Each caveola contains multiple glycosylphosphatidylinositol-anchored membrane proteins. *Cold Spring Harbor Symp. Quant. Biol.* **57**, 593-604.

Zamoyska, R., Derham, P., Gorman, S. D., von Hoegen, P., Bolen, J. B., Veillette, A. and Parnes, J. R. (1989). Inability of CD8 α' polypeptides to associate with p56^{lck} correlates with impaired function in vitro and lack of expression in vivo. *Nature* **342**, 278-81.

Zurzolo, C., Hof, W. v., Meer, G. v. and Rodriquez-Boulan, E. (1994). VIP21/caveolin, glycosphingolipid clusters and the sorting of glycosylphosphatidylinositol-anchored proteins in epithelial cells. *EMBO J.* **13**, 42-53.

(Received 13 February 1994 - Accepted 14 March 1994)